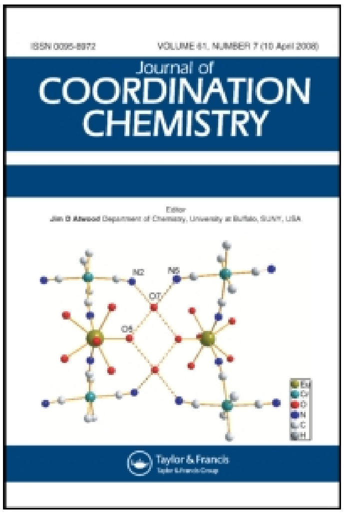

Journal of Coordination Chemistry
Publication details, including instructions for authors and subscription information:
http://www.informaworld.com/smpp/title~content=t713455674

Hydrothermal synthesis, crystal structures, and blue photoluminescence of two 2-D Ag-1,2,4-triazolate coordination polymers with $4^4 6^2$ topology

Quan-Guo Zhai[a]; Jing-Ping Niu[a]; Man-Cheng Hu[a]; Yan Wang[a]; Wen-Juan Ji[a]; Shu-Ni Li[a]; Yu-Cheng Jiang[a]
[a] Key Laboratory of Macromolecular Science of Shaanxi Province, School of Chemistry and Materials Science, Shaanxi Normal University, Xi'an, Shaanxi 710062, P.R. China

To cite this Article Zhai, Quan-Guo , Niu, Jing-Ping , Hu, Man-Cheng , Wang, Yan , Ji, Wen-Juan , Li, Shu-Ni and Jiang, Yu-Cheng(2009) 'Hydrothermal synthesis, crystal structures, and blue photoluminescence of two 2-D Ag-1,2,4-triazolate coordination polymers with $4^4 6^2$ topology', Journal of Coordination Chemistry, 62: 18, 2927 — 2936

To link to this Article: DOI: 10.1080/00958970902962782

URL: http://dx.doi.org/10.1080/00958970902962782

Journal of Coordination Chemistry
Vol. 62, No. 18, 20 September 2009, 2927–2936

Hydrothermal synthesis, crystal structures, and blue photoluminescence of two 2-D Ag–1,2,4-triazolate coordination polymers with $4^4 6^2$ topology

QUAN-GUO ZHAI*, JING-PING NIU, MAN-CHENG HU, YAN WANG, WEN-JUAN JI, SHU-NI LI and YU-CHENG JIANG

Key Laboratory of Macromolecular Science of Shaanxi Province, School of Chemistry and Materials Science, Shaanxi Normal University, Xi'an, Shaanxi 710062, P.R. China

(*Received 15 December 2008; in final form 11 February 2009*)

Two 2-D metal-organic coordination polymers, $\{[Ag(NH_2\text{–}BPT)] \cdot NO_3\}_n$ (**1**) and $\{[Ag(BPT)] \cdot H_2O\}_n$ (**2**), have been synthesized *via* self-assembly of $AgNO_3$ and 4-amino-3,5-*bis*(3-pyridyl)-1,2,4-triazole (NH_2–BPT) under hydrothermal conditions by controlling the reaction temperatures. Lower reaction temperature (140°C) led to formation of **1**, which crystallizes in the monoclinic system, space group $C2/c$, $a = 24.001(3)$, $b = 15.844(2)$, and $c = 12.981(3)$ Å, $V = 2996.8(6)$ Å^3, $Z = 8$. When the temperature was increased to 180°C, *in situ* deaminization of the organic ligand led to crystallization of **2** (space group P_21/n, $a = 7.3106(10)$, $b = 19.633(2)$, and $c = 9.0596(16)$ Å, $V = 1190.2(3)$ Å^3, $Z = 4$). The NH_2–BPT in **1** and BPT in **2** are μ_4 tetradentate utilizing two triazolyl and two pyridyl nitrogens, generating an unusual 2-D layer, in which binuclear Ag(I) motifs and organic ligands are four-connecting nodes that inter-link in $4^4 6^2$ topology. Adjacent 2-D metal-organic layers are linked by a system of hydrogen bonds to form 3-D supramolecular frameworks. Strong blue fluorescence emissions are observed for **1** and **2** in the solid state at ambient temperature.

Keywords: Silver; 3,5-*bis*(3-pyridyl)-1,2,4-triazole; Coordination polymer; Photoluminescence; Topology

1. Introduction

Design and construction of metal-organic coordination polymers have attracted interest for developing functional materials with applications in catalysis, gas absorption, nonlinear optics, ion-exchange, luminescence, magnetism, etc. [1–8]. The diversity in framework structures of such materials depends on the organic spacers and metal centers, as well as on the reaction pathways. For organic spacers, the solubility, coordination activity, length, geometry, and relative orientation of the donor groups play important roles in dictating polymer framework topology; *exo*-bidentate N,N'-dipyridine ligands are excellent rod-like connectors, forming coordination frameworks from 1- to 3-D upon metalation [5, 6, 9–14]. Modification of 4,4′-dipyridine by introducing different spacers between the terminal pyridyl groups have produced unexpected metal-organic polymeric

---

*Corresponding author. Email: zhaiqg@snnu.edu.cn

Journal of Coordination Chemistry
ISSN 0095-8972 print/ISSN 1029-0389 online © 2009 Taylor & Francis
DOI: 10.1080/00958970902962782

architectures. For example, Du [15–17] and Dong [18, 19] have focused on crystal engineering of a series of angular dipyridines, 2,5-*bis*(3-/4-pyridyl)-1,3,4-oxadiazole or 4-amino-3,5-*bis*(3-/4-pyridyl)-1,2,4-triazole. As a result of the specific geometry of such diazole- or triazole-containing ligands and the coordination preferences of transition metals, many new coordination polymers, some with open channels, interesting luminescent properties and unprecedented topologies, have been obtained [15–19]. Few coordination polymers constructed from silver centers and diazole- or triazole-containing dipyridines have been obtained to date, although Ag(I) is favorable for construction of coordination polymers because of its coordination diversity and flexibility, as well as its ability to coordinate with a variety of donor atoms [20–22].

As part of our ongoing research project dealing with coordination chemistry of 1,2,4-triazole ligands, we use hydro(solvo)thermal synthesis to discover new Ag(I)–1,2,4-triazolate complexes. We have successfully synthesized a series of Ag/1,2,4-triazole/polyoxometalate hybrid supramolecular solids [23] and a novel 3-D Ag–dmtrz (dmtrz = 3,5-dimethyl-1, 2, 4-triazole) coordination polymer with non-interpenetrating $8^2$10-a topology [24] utilizing dialkyl-substituted 1,2,4-triazole ligands. In the present study, by controlling reaction temperatures, self-assembly of $AgNO_3$ and 4-amino-3,5-*bis*(3-pyridyl)-1,2,4-triazole (NH_2–BPT) under hydrothermal conditions produced two 2-D coordination polymers, $\{[Ag(NH_2\text{–}BPT)] \cdot NO_3\}_n$ (**1**) and $\{[Ag(BPT)] \cdot H_2O\}_n$(**2**), which were characterized by elemental analysis, FT-IR, X-ray powder diffraction (XRPD), X-ray single-crystal diffraction, TG/DTA, and photoluminescence measurements. Although Dong and co-workers [18] have created three Ag–NH_2–BPT complexes using solution methods, we are reporting the first example of an Ag–BPT coordination polymer.

2. Experimental

2.1. *Materials and physical measurements*

The ligand 4-amino-3,5-*bis*(3-pyridyl)-1,2,4-triazole (NH_2–BPT) was prepared according to the literature method [25]. Other reagents and solvents employed were commercially available and used without purification. C, H, and N elemental analyses were determined on an Elementar Vario EL III elemental analyzer. The FT-IR spectra (KBr pellets) were recorded on a Nicolet Avatar 360 FT-IR spectrometer from 4000–400 cm^{-1}. Fluorescence spectra were measured on powder crystal samples at room temperature using a Cary Eclipse fluorescence spectrophotometer. The excitation slit and emission slit were both 2.5 nm. Thermal stability studies were carried out on a NETSCHZ STA-449C thermoanalyzer under nitrogen (40–1000°C) at a heating rate of 10°C min^{-1}.

2.2. *Synthesis of $\{[Ag(NH_2\text{–}BPT)] \cdot NO_3\}_n$ (1)*

A mixture containing $AgNO_3$ (0.17 g, 1.0 mmol) and NH_2–BPT (0.24 g, 1.0 mmol) in 10 mL H_2O was introduced into a Parr Teflon-lined stainless steel vessel (25 cm^3), the vessel was sealed, heated at 140°C for 5 days under autogenous pressure and cooled slowly ($5^{\circ}C\,h^{-1}$) to room temperature. Colorless block crystals were collected by filtration, washed with water and ethanol, and dried in air. Yield: 0.31 g (*ca* 76% based on Ag). Anal. Calcd (%) for $C_{12}H_{10}N_7O_3Ag$: C, 35.32; H, 2.47; N, 24.02. Found (%): C, 35.28; H, 2.49; N, 24.48. IR (solid KBr pellet in cm^{-1}): 3437(w), 3361(w), 3270(w), 3195(w), 2922(w), 1624(w), 1575(w), 1463(w), 1382(vs), 1134(w), 1023(w), 965(w), 907(w), 813(w), 710(m), and 619(w).

2.3. *Synthesis of* $\{[Ag(BPT)]\cdot H_2O\}_n$ *(2)*

The preparation of **2** is similar to that of **1** except the reaction temperature which was set at 180°C. Colorless hexagonal prism-shaped crystals of **2** were obtained after the reaction solution cooled gradually ($5^{\circ}C\ h^{-1}$), washed with water, and air-dried. Yield: 0.23 g (*ca* 65% on the base of Ag). Anal. Calcd (%) for $C_{12}H_{10}N_5OAg$: C, 41.40; H, 2.90; N, 20.12. Found (%): C, 41.68; H, 2.89; N, 20.08. IR (solid KBr pellet in cm^{-1}): 3600(s), 3300(s), 3181(w), 3060(w), 1609(m), 1566(w), 1462(m), 1418(s), 1294(w), 1169(w), 1105(w), 998(s), 934(w), 823(m), 764(m), 706(s), 620(w), 550(w), and 499(w).

2.4. *Crystal structure determination*

Suitable single crystals of **1** and **2** were carefully selected under an optical microscope and glued to thin glass fibers. Crystallographic data were collected with a Siemens Smart CCD diffractometer with graphite-monochromated Mo-Kα radiation ($\lambda = 0.71073$ Å) at $T = 293(2)$ K. Absorption corrections were made using SADABS [26]. The structures were solved using direct methods and refined by full-matrix least-squares on F^2 by using the SHELXL-97 program package [27]. All non-hydrogen atoms were refined anisotropically. Positions of the hydrogen atoms attached to carbon and oxygen were fixed at their ideal positions. Crystal data as well as details of data collection and refinement for **1** and **2** are summarized in table 1. Selected bond lengths and angles are listed in table 2.

3. Results and discussion

3.1. *Syntheses*

As depicted in scheme 1, compounds were prepared in good yields by exploiting the hydrothermal reactions of $AgNO_3$ and NH_2–BPT ligands. The conditions reported in section 2 have been optimized for yields of crystalline products. Temperature is a key factor affecting the formation of the resulting products. Hydrothermal reaction at 140°C in a molar ratio of 1 : 1 produced colorless block crystals of **1** in 76% yield. When the temperature was increased, the yield of **1** decreased and colorless hexagonal prism-shaped crystals of **2** were obtained. Almost phase-pure products were obtained at 140°C for **1** and 180°C for **2**, whereas mixtures were obtained in intermediate temperatures. The NH_2–BPT deaminized to form BPT at higher temperatures, creating the negatively-charged BPT ligand, obviating the need for a counterion. Although some hydro (solvo)thermal *in situ* ligand synthesis reactions are known [8, 28], the deaminization of the triazolate ligand reported here is, to our knowledge, unique [29].

Table 1. Crystal data and structure refinement for **1** and **2**.

Compound	**1**	**2**
Empirical formula	$C_{12}H_{10}N_7O_3Ag$	$C_{12}H_{10}N_5OAg$
Formula weight	408.14	348.12
Crystal system	Monoclinic	Monoclinic
Space group	$C2/c$	$P_{2}1/n$
Unit all dimensions (Å, °)		
a	24.001(3)	7.3106(10)
b	15.844(2)	19.633(2)
c	8.3160(10)	9.0596(16)
α	90	90
β	108.623(2)	113.748(2)
γ	90	90
V (Å^3)	2996.8(6)	1190.2(3)
Z	8	4
$F(000)$	1616	688
ρ (Mg m^{-3})	1.809	1.943
Absorption coefficient (mm^{-1})	1.372	1.692
θ for data collection (°)	1.57–25.00	2.07–25.00
Reflections collected/unique	7412/2623	6074/2096
Unique reflections (R_{int})	0.0179	0.0183
Parameters	236	172
Goodness-of-fit on F^2	1.082	1.032
$R_1{}^a$, wR_2 [$I > 2\sigma(I)$]	0.0636, 0.2069	0.0376, 0.1675
R_1, wR_2 (all data)	0.0782, 0.2299	0.0415, 0.1747

$^aR_1 = \sum(|F_o| - |F_c|)/\sum|F_o|$, $wR_2 = [\sum w(F_o^2 - F_c^2)^2/\sum w(F_o^2)^2]^{0.5}$.

Table 2. Selected bond lengths (Å) and angles (°) for **1** and **2**.

1			
Ag(1)–N(1)	2.313(6)	Ag(1)–N(5)#2	2.366(8)
Ag(1)–N(2)#1	2.322(6)	Ag(1)–N(6)	2.398(7)
N(1)–Ag(1)–N(2)#1	110.5(2)	N(1)–Ag(1)–N(6)	125.8(2)
N(1)–Ag(1)–N(5)#2	96.6(2)	N(2)#1–Ag(1)–N(6)	98.3(2)
N(2)#1–Ag(1)–N(5)#2	115.9(3)	N(5)#2–Ag(1) –N(6)	111.1(2)
2			
Ag(1)–N(1)#1	2.269(4)	Ag(1)–N(4)	2.433(4)
Ag(1)–N(2)#2	2.280(4)	Ag(1)–N(5)	2.477(4)
N(1)#1–Ag(1)–N(2)#2	118.64(14)	N(1)#1–Ag(1)–N(5)	103.91(13)
N(1)#1–Ag(1)–N(4)	117.84(14)	N(2)#2–Ag(1)–N(5)	115.64(14)
N(2)#2–Ag(1)–N(4)	104.42(13)	N(4)–Ag(1)–N(5)	94.17(14)

Symmetry transformations used to generate equivalent atoms: **1:** #1 $-x+1/2, -y+1/2, -z+2$; #2 $x, -y+1, z+1/2$. **2:** #1 $-x+1, -y+1, -z+1$; #2 $-x, -y+1, -z+1$.

3.2. *Description of crystal structures*

X-ray single-crystal diffraction analysis shows that **1** crystallizes in the monoclinic space group $C2/c$, and the asymmetric unit consists of one Ag^+ ion, one NH_2–BPT ligand, and one NO_3^- ion. The NH_2–BPT is *cisoid* configuration and serves as μ_4-bridge *via* two triazolyl N atoms and two pyridyl N donors. The dihedral angles between the central triazole ring and two 3-pyridines are about 45 and 65°, comparable to those found in other structurally characterized complexes with *cisoid*-NH_2–BPT ligands [17]. As shown in figure 1(a), the tetrahedral Ag(1) center is defined by two triazolyl $N_{(1)}$ or $N_{(2)}$ atoms

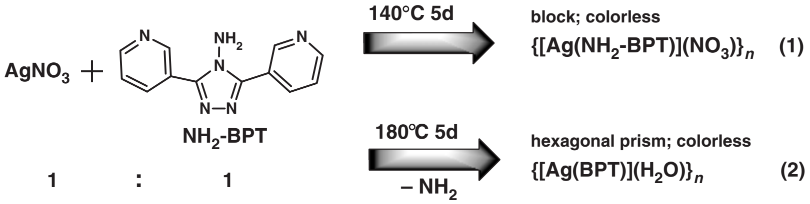

Scheme 1. The synthesis method for compounds **1** and **2**.

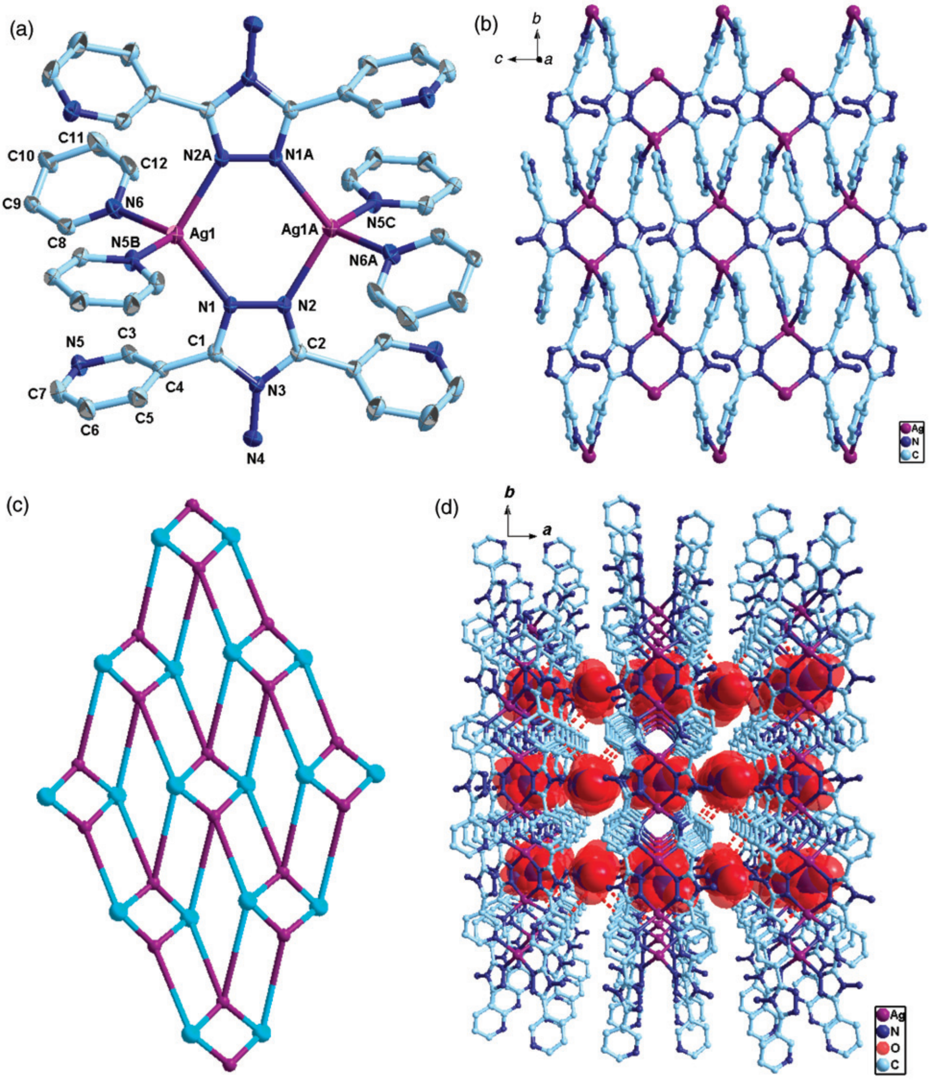

Figure 1. (a) ORTEP diagram of **1** showing the local coordination environment of Ag(I) cluster and 30% thermal ellipsoids. [Symmetry codes, A: $0.5-x, 0.5-y, 2-z$; B: $x, 1-y, 0.5+z$; C: $0.5-x, -0.5+y, 1.5-z$]. (b) View of the 2-D metal-organic network of **1**. (c) The 2-D topological representation of **1**. (d) View of the 3-D supramolecular framework of **1** generated by metal-organic nets and disorder NO_3^- counterions *via* the C–H $\cdots$ O weak hydrogen bonds (broken lines).

from different NH_2–BPT ligands and two pyridine donors from two other NH_2–BPT ligands with Ag–N distances and N–Ag–N angles of 2.313(6)–2.398(7) Å and 96.6(2)–125.8(2)°. Two metal centers are connected by two triazoles *via* pyrazole-like bridging to generate a $[Ag_2N_4]$ binuclear cyclic unit with Ag···Ag separation of 4.0227(10) Å. A pair of NH_2–BPT ligands link two Ag centers through four pyridine nitrogens into a large $[Ag_2(NH_2\text{–}BPT)_2]$ ring, which leads to longer Ag···Ag separation of 11.8267(17) Å. The two cyclic motifs inter-linked to generate a 2-D network of **1** in the *b*,*c*-plane (figure 1b). In order to analyze the net, we define the silver center and NH_2–BPT as two kinds of four-connected nodes. These two equivalent nodes lead to an unusual network topology depicted in figure 1(c). The short and long Schläfli symbols for this net are $4^4 6^2$ and 4.4.4.4, respectively. The node–node distances are 3.4596(6), 3.4546(6), 6.798(10), and 6.5482(9) Å. Further, if the dinuclear Ag_2 motif is regarded as node and NH_2–BPT as linker, this 2-D layer can be further simplified as a 6-connected 3^6 network with the node–node distances of 8.9469(9) and 15.844(2) Å. There exist 8 × 8 Å cavities in the 2-D network when viewed towards the plane [2 0 1], in which disordered NO_3^- are located. Thus, the 2-D metal-organic layers are extended into the final 3-D supramolecular frameworks, as depicted in figure 1(d), through C–H···O weak hydrogen bonds (the distances between proton and oxygen in the range of 2.47–2.57 Å).

Deaminization of triazolate ligands at higher temperature led to formation of a similar structure for **2**, which crystallizes in the monoclinic space group $P2_1/n$. Complex **2** consists of one anionic BPT ligand, one Ag^+ ion, and one crystallization H_2O molecule in the crystallographically asymmetric independent unit. Just NH_2–BPT in **1**, BPT takes the *cisoid* configuration as a μ_4-bridge to coordinate four silver cations. The dihedral angles between the central triazole ring and two 3-pyridines are 26 and 30°, markedly smaller than those in **1**. Each Ag(I) has tetrahedral geometry, coordinated to four N donors from two triazole and two 3-pyridines of four different BPT ligands (Ag–N = 2.269(4)–2.477(4) Å and N–Ag–N = 94.17(14)–118.64(14)°) (figure 2a). Like the linkage between metal centers and organic ligands in **1**, two M–L cyclic rings are also observed, $[Ag_2(\text{triazole})_2]$ and $[Ag_2(\text{BPT})_2]$, with Ag···Ag distances of 3.6993(8) and 12.8861(23) Å, respectively. The 2-D network of **2** generated by these two types of cyclic motifs extends along the *a*,*c*-plane (figure 2b), which can be simplified as the same 2-D topological net as for **1**, with different node–node distances (6.7955(12), 6.7591(10), 3.4219(5), and 3.4310(5) Å). Strong aromatic π–π stacking interactions between 3-pyridyl rings are observed in this layer with a center–to–center distance of about 3.7 Å, which further stabilizes this 2-D network. Crystallization waters are trapped in the cavity (6 × 6 Å) of 2-D layers, linking adjacent layers into the 3-D supramolecular framework of **2** (figure 2c) through O–H···N (O(1)···N(3) 2.9201(1) Å) and C–H···O (C(11)···O(1) 3.2938(2) Å) hydrogen bonding systems. Different from **1**, the 2-D metal-organic layers are packed in an ABAB interlaced mode.

3.3. *XRPD, TGA, and photoluminescence properties*

Compounds **1** and **2** were characterized *via* X-ray powder diffraction (XPRD) at room temperature (Supplementary material). The XPRD patterns measured for synthesized samples were in good agreement with the XPRD patterns simulated from the respective single-crystal X-ray data. These results indicate the purity of **1** and **2**.

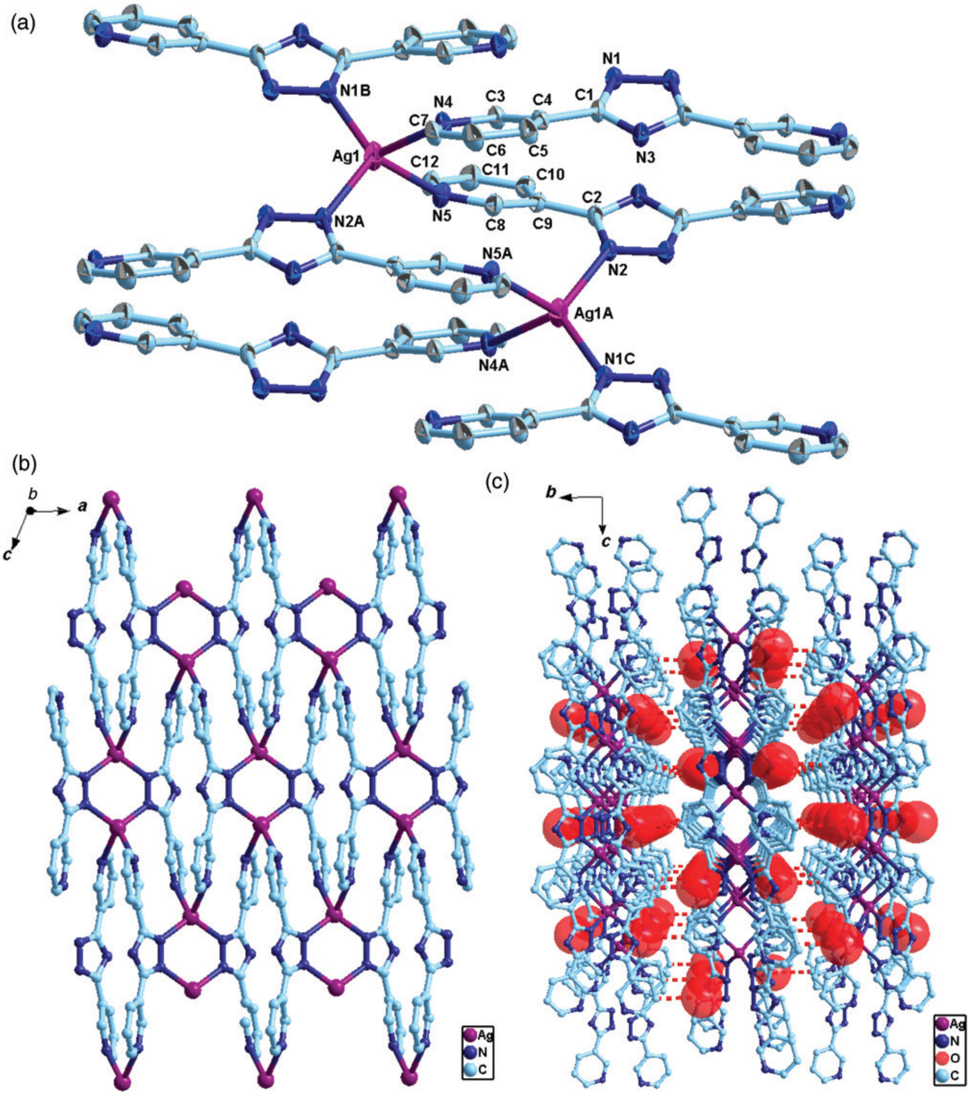

Figure 2. (a) ORTEP diagram of **2** showing the local coordination environment of Ag(I) cluster and 30% thermal ellipsoids. [Symmetry codes, A: $-x, 1-y, 1-z$; B: $1-x, 1-y, 1-z$; C: $-1+x, y, z$]. (b) View of the 2-D metal-organic network of **2**. (c) View of the 3-D supramolecular framework of **2** generated by metal-organic nets and crystalline water molecules *via* hydrogen bonds (broken lines).

Since thermal stability of metal-organic framework material is an important quality for application purposes, compounds **1** and **2** were studied by thermal analysis in nitrogen from 40 to 1000°C (Supplementary material). Their TG curves support their chemical compositions. The weight loss curve of **1** showed that it was stable at *ca* 275°C. Over the range 275–800°C, a series of continuous weight losses were due to the decomposition of NH_2–BPT ligands and NO_3^-; the residue was Ag_2O (experimental 29.1%; Calcd 28.4%). For **2**, the weight loss of 5.6% from 40 to 225°C corresponds to release of crystalline water (Calcd 5.2%). The 2-D Ag–BPT network was stable at *ca* 350°C; above 350°C, a sharp weight loss occurred, ending at about 850°C, indicating

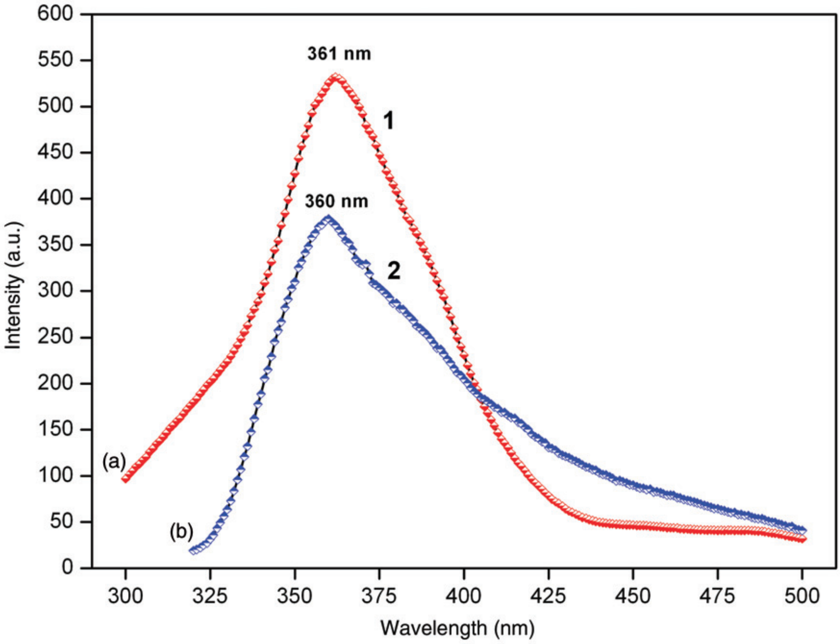

Figure 3. Solid state emission spectra of **1** (a) and **2** (b) at ambient temperature.

complete decomposition of organic ligands and the residual composition of Ag_2O (experimental 33.0%; Calcd 33.3%).

Syntheses of metal-organic coordination polymers by judicious choices of conjugated organic spacer and transition metal centers can be an efficient method to obtain electroluminescent materials, especially for d^{10} or d^{10}–d^{10} systems. The luminescent properties of several M–1,2,4-triazolate polynuclear compounds or coordination polymers indicate that emission colors of organic spacers were remarkably affected by their incorporation into metal coordination compounds [18, 30–34]. Thus, we investigated the photoluminescence of **1** and **2** in the solid state under room temperature. As shown in figure 3, upon excitation of the solid samples at $\lambda = 260$ nm, intense bonds in the emission spectra are observed at 361 nm for **1** and 360 nm for **2**. As reported by Dong and co-workers [18], similar emission bonds were also observed for the organic ligands. Thus, luminescence of **1** and **2** is tentatively assigned to intraligand fluorescent emissions. Compared with organic ligands, the enhancement and marked blue-shifts are due to coordination to the Ag center increasing the ligand conformational rigidity and reducing the non-radiative decay of the intraligand ($\pi - \pi^*$) excited state [35, 36].

4. Conclusion

By controlling the temperature of hydrothermal reactions, two 2-D Ag(I)–1,2,4-triazolate coordination polymers with $4^4 6^2$ topology were synthesized and characterized. Further investigation on Ag–1,2,4-triazolate metal-organic frameworks is currently underway in our lab.

Supplementary material

Crystallographic data have been deposited with the Cambridge Crystallographic Data Centre (CCDC) (Email: deposit@ccdc.cam.ac.uk) as supplementary materials and the CCDC reference numbers for **1** and **2** are 712128 and 712129, respectively.

Acknowledgements

This work was supported by the National Natural Science Foundation of China (Grant Nos 20801033 and 20871079) and the Youth Foundation of Shaanxi Normal University.

References

[1] S.R. Batten, R. Robson. *Angew. Chem., Int. Ed.*, **37**, 1460 (1998).
[2] M. Eddaoudi, D.B. Moler, H. Li, B. Chen, T. Reineke, M. O'Keeffe, O.M. Yaghi. *Acc. Chem. Res.*, **34**, 319 (2001).
[3] B. Moulton, M.J. Zaworotko. *Chem. Rev.*, **101**, 1629 (2001).
[4] O.R. Evans, W. Lin. *Acc. Chem. Res.*, **35**, 511 (2002).
[5] S.R. Batten, K.S. Murray. *Coord. Chem. Rev.*, **246**, 103 (2003).
[6] S. Kitagawa, R. Kitaura, S. Noro. *Angew. Chem., Int. Ed.*, **43**, 2334 (2004).
[7] N.W. Ockwig, O. Delgado-Friedrichs, M. O'Keeffe, O.M. Yaghi. *Acc. Chem. Res.*, **38**, 176 (2005).
[8] X.M. Chen, M.L. Tong. *Acc. Chem. Res.*, **40**, 162 (2007).
[9] O.M. Yaghi, H. Li. *J. Am. Chem. Soc*, **118**, 295 (1996).
[10] S. Noro, R. Kitaura, M. Kondo, S. Kitagawa, T. Ishii, H. Matsuzaka, M. Yamashita. *J. Am. Chem. Soc.*, **124**, 2568 (2002).
[11] X.L. Wang, C. Qin, E.B. Wang, Y.G. Li, Z.M. Su, L. Xu, L. Carlucci. *Angew. Chem., Int. Ed.*, **44**, 5824 (2005).
[12] M.H. Zeng, W.X. Zhang, X.Z. Sun, X.M. Chen. *Angew. Chem., Int. Ed.*, **44**, 3079 (2005).
[13] W.G. Lu, C.Y. Su, T.B. Lu, L. Jiang, J.M. Chen. *J. Am. Chem. Soc.*, **128**, 34 (2006).
[14] J. Zhang, R. Liu, P. Feng, X. Bu. *Angew. Chem., Int. Ed.*, **46**, 8388 (2007).
[15] M. Du, Z.H. Zhang, X.J. Zhao, Q. Xu. *Inorg. Chem.*, **45**, 5785 (2006).
[16] M. Du, Z.H. Zhang, L.F. Tang, X.G. Wang, X.J. Zhao, S.R. Batten. *Chem.-Eur. J.*, **13**, 2578 (2007).
[17] M. Du, Z.H. Zhang, Y.P. You, X.J. Zhao. *Cryst. Eng. Comm.*, **10**, 306 (2008) and references cited therein.
[18] Y.B. Dong, H.Y. Wang, J.P. Ma, R.Q. Huang. *Cryst. Growth Des.*, **5**, 789 (2005) and references cited therein.
[19] Y.B. Dong, T. Sun, J.P. Ma, X.X. Zhao, R.Q. Huang. *Inorg. Chem.*, **45**, 10613 (2006).
[20] P.C. Ford, A. Vogler. *Acc. Chem. Res.*, **26**, 220 (1993).
[21] T. Sun, K. Seff. *Chem. Rev.*, **94**, 857 (1994).
[22] C.A. Tsipis, E.E. Karagiannis, P.F. Kladou, A.C. Tsipis. *J. Am. Chem. Soc.*, **126**, 12916 (2004).
[23] Q.G. Zhai, X.Y. Wu, S.M. Chen, Z.G. Zhao, C.Z. Lu. *Inorg. Chem.*, **46**, 5046 (2007).
[24] Q.G. Zhai, M.C. Hu, S.N. Li, Y.C. Jiang. *Inorg. Chim. Acta*, **362**, 1355 (2009).
[25] R.M. Herbst, J.A. Garrison. *J. Org. Chem.*, **18**, 872 (1953).
[26] G.M. Sheldrick. *SADABS*, *Program for Area Detector Adsorption Correction*, Institute for Inorganic Chemistry, University of Göttingen, Germany (1996).
[27] G.M. Sheldrick. *SHELXL*-97, *Program for Solution of Crystal Structures*, University of Göttingen, Germany (1997).
[28] X.M. Zhang. *Coord. Chem. Rev.*, **249**, 1201 (2005).
[29] Z.G. Zhao, J. Zhang, X.Y. Wu, Q.G. Zhai, L.J. Chen, S.M. Chen, Y.M. Xie, C.Z. Lu. *Cryst. Eng. Comm.*, **10**, 273 (2008).
[30] J.P. Zhang, Y.Y. Lin, X.C. Huang, X.M. Chen. *J. Am. Chem. Soc.*, **127**, 5495 (2005).
[31] Y.B. Dong, J.Y. Cheng, H.Y. Wang, R.Q. Huang, B. Tang, M.D. Smith, H.C. Zur Loye. *Chem. Mater.*, **15**, 2593 (2003).

[32] Y.B. Dong, J.Y. Cheng, R.Q. Huang, B. Tang, M.D. Smith, H.C. Zur Loye. *Inorg. Chem.*, **42**, 5699 (2003).
[33] Q.G. Zhai, M.C. Hu, S.N. Li, Y.C. Jiang. *Inorg. Chem. Commun.*, **11**, 1147 (2008).
[34] W. Ouellette, B.S. Hudson, J. Zubieta. *Inorg. Chem.*, **46**, 4887 (2007).
[35] B. Ding, L. Yi, Y. Wang, P. Cheng, D.Z. Liao, S.P. Yan, Z.H. Jiang, H.B. Song, H.G. Wang. *Dalton Trans.*, 665 (2006).
[36] Y.Q. Huang, B. Ding, H.B. Song, B. Zhao, P. Ren, P. Cheng, H.G. Wang, D.Z. Liao, S.P. Yan. *Chem. Commun.*, 4906 (2006).